



# An Intelligent UAV based Data Aggregation Algorithm for 5G-enabled Internet of Things

Xiaoding Wang<sup>a</sup>, Sahil Garg<sup>b</sup>, Hui Lin<sup>a,\*</sup>, Georges Kaddoum<sup>b</sup>, Jia Hu<sup>c,\*</sup>, Mohammed F. Alhamid<sup>d</sup>

<sup>a</sup> College of Mathematics and Informatics, Fujian Normal University, Fuzhou, Fujian, 350117, China

<sup>b</sup> École de technologie supérieure (ETS), Montreal, Canada

<sup>c</sup> University of Exeter, UK

<sup>d</sup> Chair of Smart Technologies, College of Computer and Information Sciences, King Saud University, Riyadh 11543, Saudi Arabia

## ARTICLE INFO

### Keywords:

Unmanned Aerial Vehicle  
5G  
Internet of Things  
Data aggregation  
Deep reinforcement learning

## ABSTRACT

Unmanned Aerial Vehicle (UAV) has become a significant part of 5G or beyond 5G (B5G) paradigm, and is used in various scenarios, including cargo delivery, agricultural application, event surveillance, etc. Although plenty of studies have been proposed on UAV-based data aggregation, how to ensure security and energy-efficiency of the data aggregation process in 5G-enabled Internet of Things (IoT) is an open problem. In this paper, we propose an Intelligent UAV-based Data Aggregation Algorithm, named IDAA for 5G-Enabled IoT. Specifically, IDAA applies v-Support Vector Regression (v-svr) to predict the data collection rate. Then, a security level based task decomposition mechanism is designed that allows UAVs to accept the tasks of corresponding security levels. Finally, energy efficient routes for UAV are planned utilizing a deep reinforcement learning method to achieve the trade-off between the sinking ratio and the energy cost. The theoretical analysis and simulation results indicate that (i) IDAA improves the security of data aggregation; and (ii) IDAA enables UAVs to collect more data and consume less energy compared with baseline strategies.

## 1. Introduction

Unmanned Aerial Vehicle (UAV), aka drone, can perform specific aviation tasks by controls through wireless channels. Drones are currently widely used in various social fields, bringing great changes to our work and life, i.e., drone broadcasting pesticide, drone logistics, drone filming, drone light show, etc. UAVs are mainly controlled by human through wireless communications, e.g., Wi-Fi and Bluetooth. However, the communication distance of Wi-Fi or Bluetooth is short. For example, the control supported by either Wi-Fi or Bluetooth is limited within the visual range of 300~500 m such that the flying range of UAVs is greatly restricted. Compared with Wi-Fi, 4G/5G technologies have a wider coverage, which will make UAV communications more flexible and reliable.

The communication between the UAV and the ground serves mainly three purposes: image transmission, digital transmission and remote control. 4G LTE cellular communication can provide image transmission with the resolution of 1280 × 720. However, in some specific scenarios, i.e., facial recognition, it still cannot meet the needs of users. Theoretically, 5G can reach the bandwidth of up to 20 Gbps. That indicates UHD videos of 4K or 8K resolution can be supported

perfectly with 5G. Compared to traditional ground cameras with the static and low-latitude view with 4G, the view of drones supported by 5G is dynamic, wide-angle, ultra-high-definition and high-latitude. In addition, ultra-low latency of 5G can achieve the transmission delay on millisecond-level. All these characteristics contribute to fast response and accurate control for drones. On the other hand, the positioning accuracy of 5G, which reaches centimeter-level, exceeds that of both LTE and GPS such that the needs of flying over complex terrains of urban areas are met.

Previous studies on UAV-based data aggregation in 5G-enabled IoT fail to ensure both security and energy-efficiency of the data aggregation process. To address this problem, an Intelligent UAV-based Data Aggregation Algorithm (IDAA) is proposed for 5G enabled IoT in this paper. Specifically, IDAA consists of an v-support vector regression (v-SVR) based data collection rate (DCR) prediction algorithm, a security level based task decomposition scheme, and a deep reinforcement learning (DRL) based UAV route design algorithm. Our contributions are specified as follows.

1. To improve the security of data aggregation, IDAA adopts the security level based task decomposition, i.e., each UAV is restricted

\* Corresponding authors.

E-mail addresses: [wangdin1982@fjnu.edu.cn](mailto:wangdin1982@fjnu.edu.cn) (X. Wang), [sahil.garg@ieee.org](mailto:sahil.garg@ieee.org) (S. Garg), [linhui@fjnu.edu.cn](mailto:linhui@fjnu.edu.cn) (H. Lin), [georges.kaddoum@etsmtl.ca](mailto:georges.kaddoum@etsmtl.ca) (G. Kaddoum), [j.hu@exeter.ac.uk](mailto:j.hu@exeter.ac.uk) (J. Hu), [mohalhamid@ksu.edu.sa](mailto:mohalhamid@ksu.edu.sa) (M.F. Alhamid).

<https://doi.org/10.1016/j.comnet.2020.107628>

Received 21 July 2020; Received in revised form 27 September 2020; Accepted 17 October 2020

Available online 5 November 2020

1389-1286/© 2021 Elsevier B.V. All rights reserved.

to accept a task of a specific security level inferior to that of the UAV. That suggests the higher security level a task possesses the less UAVs are allowed to access the task. Besides, a UAV of a higher security level has a less chance to expose the sensitive information contained in the task.

2. To ensure the energy efficiency of data aggregation, IDAA applies a Deep Reinforcement Learning (DRL) technology, DQN, to design UAV routes considering the sinking ratio and the energy cost. Note that the energy cost of a route is calculated based on risks and elevations of realistic terrains, i.e., flying over a high mountain or a dense forest is risky while it is easy to travel through a flat of low attitude.
3. The theoretical analysis and simulation results shows that (i) IDAA improves the security of data aggregation; and (ii) IDAA ensures UAVs to collect more data and consume less energy cost compared with contemporary strategies.

We organize the remainder of this paper as follows. The related work is given in Section 2. We introduce the system model in Section 3. The implementation detail of proposed IDAA is presented in Section 4. Section 5 presents the validation experiments. We conclude this paper in Section 6.

## 2. Related work

The UAV based data aggregation in 5G-enabled IoT has drawn a great attention in recent years with plenty of works proposed.

The data aggregation route design has been studied for years. In [1], hyperedges of hypergraph are adopted for data aggregation route design utilizing Delaunay triangulation. In [2], efficient clustering is employed to equalize energy cost. In [3], relays are exploited to shorten the data aggregation route. In the real environment, terrains affect energy cost much more than route length. In [4], the energy cost is reduced utilizing stochastic geometry. In [5], the energy efficient clustering is developed to reduce the energy cost meanwhile more data is collected. In [6], Abbas and Younis convex hulls are employed for data aggregation and relays are deployed for communication reestablishment. In [7], a hybrid method is developed for data aggregation and energy saving. In [8], terrain influences are quantified utilizing grid based technology to discover minimum energy cost routes. In [9], radial bias function neural network is applied to predict the data collection rate for a better data aggregation route design. In [10], the Deep Q-Network (DQN) is utilized to design a simulation system with the consideration of 3D environment and different events distributions.

The drone location problem of the minimum cost is discussed in [11]. Tuba et al. [12] aims to maximize the coverage of drones on monitored area by discovering the optimal positions. Shakhateh et al. [13] focus on maximizing the uplink transmission time by locating optimal positions of UAVs. In [14], Rodriguez et al. try to solve the traffic problem of drones in both routing and wavelength for drones. Note that previous work cannot achieve the trade-off between the sinking ratio and the energy cost.

Although plenty of works have been proposed for UAV-based data aggregation in 5G-enabled IoT, there are still two problems: (I) how to restrict UAVs to collect data from sensors of corresponding security levels; and (II) how to increase the sinking ratio meanwhile decrease the energy cost. In this paper, an Intelligent UAV-based Data Aggregation Algorithm (IDAA), is proposed to address these two problems.

## 3. System model

In this paper, a 5G-enabled IoT network with a set of data aggregation tasks with different security levels are considered. Specifically, the network is deployed with a set of sensors  $S = \{s_i\}$ , each of which is responsible for collecting sensitive information. That suggests we can partition sensors into clusters  $C_s$  such that each cluster of sensors have

a certain security level. The UAVs are then assigned to aggregate data from sensors under the constrain that the security level of the UAV should be higher than that of the sensor. On the other hand, the energy cost of the data aggregation should be considered due to the realistic terrains will affect the energy cost of UAV. As a promising technology in Machine Learning, DRL has been applied to tackle various challenging problems in UAV [15], edge computing [16,17], IoT [18,19], etc. In this paper, the UAV flying route is developed utilizing the deep reinforcement learning algorithm DQN.

It is worth to mention that the energy cost consists of two parts, i.e., the energy consumed by both receiving and transmitting data, and the energy required within the data collection path that depends on the velocity and different flight stages including acceleration, deceleration, hovering, and turning. We use the energy model proposed by Ding et al. [20] to quantify the effect of velocity on UAV energy consumption during the flight.

1. *Velocity*: If the drone is flying in a straight line at different speeds, i.e., 2 m/s, 4 m/s, 6 m/s and 8 m/s, then the power consumption will be 242 W, 245 W, 246 W, and 268 W, respectively.
2. *Acceleration and Deceleration*: The energy consumption of a drone mainly depends on the power consumption while accelerating or decelerating. The power consumption increases as the velocity and vice versa during the acceleration and deceleration which are similar to that described in the effect of velocity.
3. *Turning*: The power consumption of a drone is considered while rotating at angles with the increment of  $45^\circ$ . The power consumption  $P_{turn}$  equal to 260 W when angular speed  $v_{turn}$  reaches 2.07 rad/s. Then, the energy consumption during turn  $Energy_{turn}$  is given by

$$Energy_{turn} = \Lambda_\theta P_{turn} / v_{turn} \quad (1)$$

where  $P_{turn}$  denotes the power consumption,  $\Lambda_\theta$  denotes turning angle,  $v_{turn}$  represents angular velocity while turning.

4. *Flying Straight*: If a drone is flying along a straight-line, then apart from flying at uniform speed the acceleration and deceleration are considered. Then the energy cost  $Energy_{v,d}$  is then calculated as

$$Energy_{v,d} = \int P_{acc} dt + Energy_T + \int P_{dec} dt \quad (2)$$

where acceleration power consumption is denoted by  $P_{acc}$ , deceleration power consumption is denoted by  $P_{dec}$ ,  $Energy_T$  denotes the energy consumption considering terrain influences, and the travel distance is represented by  $d$ .

And we adopt the grid based terrain quantification for energy cost calculation. Let  $r_c$ ,  $e_c$ , and  $d_c$  denote the risk, elevation and distance respectively. Then, the weight  $\omega_c$  of cell  $c$  is given by

$$\omega_c = \int_{d_c} \int_{e_c} r_c, \quad (3)$$

For a route  $T$ , we then compute the energy consumption caused by terrain  $Energy_T$  as

$$Energy_T = \mu \sum_{c \in T} \omega_c, \quad (4)$$

where  $\mu$  represents the energy coefficient.

On the other hand, the energy cost for communication between drones and buoys consists of that of receiving  $Energy_{rec}$  and transmitting  $Energy_{tra}$  of data, which is given by

$$Energy_{tra} = \begin{cases} p_s * (Energy_c + Energy_s * d^2) & \text{if } d_0 > d \\ p_s * (Energy_c + Energy_t * d^4) & \text{if } d_0 \leq d \end{cases} \quad (5)$$

$$Energy_{rec} = p_s * Energy_c$$

where the energy dissipation on the circuitry of receiver or transmitter is denoted by  $Energy_c$ , the packet size is denoted by  $p_s$ ,  $d_0$  is a pre-determined threshold,  $Energy_s$  and  $Energy_t$  denote the energy cost on

amplifier for short or long distance transmission of one bit, respectively. Thereby, for the  $i$ th drone, the energy cost  $Energy_{i,T}$  is then calculated by

$$Energy_{i,T} = Energy_{tra} + Energy_{rec} + Energy_{turn} + Energy_{v,d}. \quad (6)$$

Note that if a drone is surrounded by a number of sensors, then how to choose a position to efficiently collect data remains a challenge. According to energy consumption model (6), which is a convex function, by taking the gradient to 0 the centroid position of that of all sensors is established. That suggests the drone will hover until all data is collected once it arrives at the center position. On the other hand, if a drone is flying toward a sensor only, then the communication will be established once the drone reaches the communication range of that sensor.

#### 4. The implementation details of IDAA

##### 4.1. Data collection rate prediction

The v-Support Vector Regression (v-SVR) is applied to predict data collection rate  $DCR$  prediction. Compared with traditional support vector regression, the v-SVR can reduce the amount of calculation through slack variables w.r.t the value of  $v$ , while maintaining a high predicting accuracy. At first, a linear function of  $DCR$  with respect to historical data  $x_i$  is constructed as  $DCR = (w \cdot x_i) + b$ . Note that the historical data  $x_i$  is a  $n$ -tuple with each dimension indicating the relevant information of historical data aggregation, i.e., temperature, wind speed, humidity, time, the amount of data collected, etc. Once enough historical data is collected, we can use the v-SVR to predict new data collection rate. Then, v-SVR is trained using following equations for complexity reduction.

$$\min \frac{1}{n} \sum_{i=1}^n |DCR - f(x_i)|_\epsilon + \frac{1}{2} \|w\|^2 \quad (7)$$

Furthermore, we further reduce the computational complexity by

$$\min \frac{1}{2} \|w\|^2 + \mathcal{M}[v\epsilon + \frac{1}{n} \sum_{i=1}^n (\zeta_i + \zeta_i^*)] \quad (8)$$

$$s.t. \begin{cases} \zeta_i^* \geq 0, \epsilon \geq 0 \\ DCR - (wx_i + b) \leq \epsilon + \zeta_i^*, \\ (wx_i + b) - DCR \leq \epsilon + \zeta_i. \end{cases}$$

Accordingly, the Lagrangian  $L(w, b, \gamma^{(*)}, \rho, \zeta^{(*)}, \epsilon, \rho^{(*)})$  is constructed as

$$\begin{aligned} L(w, b, \gamma^{(*)}, \rho, \zeta^{(*)}, \epsilon, \rho^{(*)}) = & -\rho\epsilon - \sum_{i=1}^n (\rho_i \zeta_i + \rho_i^* \zeta_i^*) \\ & - \sum_{i=1}^n \gamma_i^* (\zeta_i^* + (w \cdot x_i) + b - DCR + \epsilon) \\ & + \frac{1}{2} \|w\|^2 + \mathcal{M}v\epsilon + \frac{\mathcal{M}}{n} \sum_{i=1}^n (\zeta_i + \zeta_i^*) \\ & - \sum_{i=1}^n \gamma_i (\zeta_i + DCR - (w \cdot x_i) - b + \epsilon) \end{aligned} \quad (9)$$

Therefore, the derivative over  $w, \epsilon, b, \zeta_i^{(*)}$  equals to 0 results in:

$$\begin{cases} \sum_{i=1}^n (\gamma_i^* - \gamma_i) = 0 \\ \frac{\mathcal{M}}{n} - \gamma_i^{(*)} - \rho_i^{(*)} = 0 \\ w = \sum_{i=1}^n (\gamma_i^* - \gamma_i) x_i \\ \mathcal{M} \cdot v - \sum_{i=1}^n (\gamma_i + \gamma_i^*) - \rho = 0 \end{cases} \quad (10)$$

Then, v-SVR based DCR prediction can be obtained as:

$$\begin{aligned} \max. \quad & -\frac{1}{2} \sum_{i,j=1}^n (\gamma_i^* - \gamma_i)(\gamma_j^* - \gamma_j) \mathcal{K}(x_i, x_j) \\ & + \sum_{i=1}^n (\gamma_i^* - \gamma_i) DCR, \\ s.t. \quad & \begin{cases} \sum_{i=1}^n (\gamma_i^* + \gamma_i) \leq \mathcal{M} \cdot v, \\ \sum_{i=1}^n (\gamma_i^* - \gamma_i) = 0, \\ \gamma_i^{(*)} \in [0, \frac{\mathcal{M}}{n}], \end{cases} \end{aligned} \quad (11)$$

where  $\mathcal{K}(\cdot, \cdot)$  represents a nonlinear mapping. Specifically, we implement the nonlinear mapping with the Gaussian kernel function by mapping the finite-dimensional data to high-dimensional space, in which data is linearly separable. Eventually, DCR is calculated by the v-SVR as

$$DCR = \sum_{i=1}^n (\gamma_i^* - \gamma_i) \mathcal{K}(x_i, x) + b. \quad (12)$$

##### 4.2. Security level and energy efficiency based task partition

For  $N_u$  optimal routes design of UAVs, we partition the set  $S = \{s_i\}$  of sensors into clusters  $C_i$ s, in which the Hamilton cycle  $H_{C_i}$  is used as an UAV route of corresponding security levels. Further, for energy efficiency, the time between two visits of the same sensor is less than that of filling a buffer  $BUF_{s_i}$ , as

$$\frac{L(H_{C_i})}{v} \leq \frac{BUF_{s_i}}{DCR_{s_i}} (1 + \psi). \quad (13)$$

Note that the sinking ratio is at least  $\frac{1}{1+\psi}$  if (13) is satisfied. Therefore, we aim to find the optimal partition  $P = \{C_i\}$ , in which each  $H_{C_i}$  is a UAV route to meet (13). We give a four-step greedy searching algorithm to discover the optimum partition  $P$ .

Step 1, the Hamilton cycle  $H_S$  is built on set  $S$ , then sequentially marked  $s_i \in H_S$  w.r.t the  $H_S$ ;

Step 2, take the  $C_j = \{s_k\}$  as a start, then  $s_{k+1}$  is add repeatedly for  $C_j$  expansion, i.e.,  $C_j = C_j \cup s_{k+1}$ , if (13) is satisfied on each  $s_i \in C_j$  and  $s_{k+1}$ ; then repeat this step with  $s_{l+1}$  as a starter;

Step 3, take  $s_{k+1}$  sequentially as a starter to repeat step 2.

Step 4, there are many partitions established by taking previous steps, the optimum grouping  $P_i$  is discovered to satisfy the following constrains:

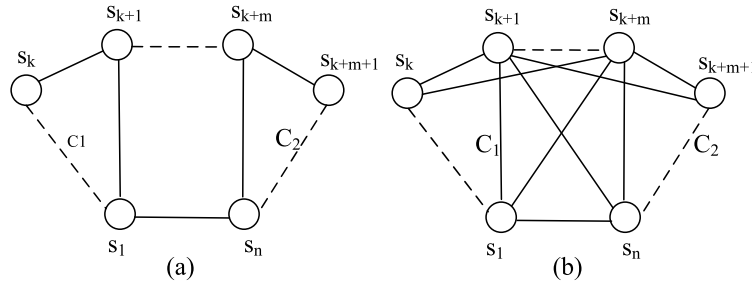
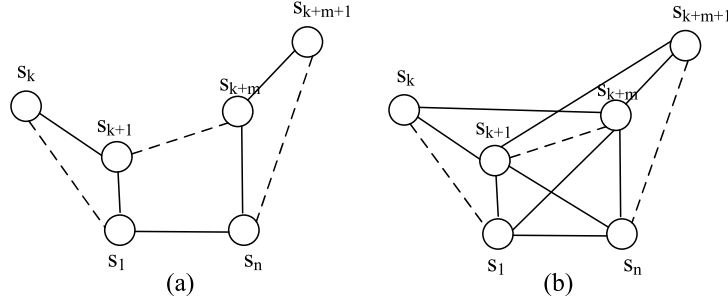
$$\begin{aligned} \min \quad & L(P_i) \\ s.t. \quad & 1. P_i = \cup C_j, \\ & 2. \forall C_k, C_j \in P_i, \exists C_k \cap C_j = \emptyset. \end{aligned} \quad (14)$$

And the proper data loss rate  $\eta$  is given by

$$\eta = \frac{L(H_{C_j}) * DCR_{s_i}}{V * BUF_{s_i}} - 1. \quad (15)$$

Note that although Eq. (15) gives the calculation of the data loss rate  $\eta$  to ensure the sinking ratio of  $\frac{1}{1+\psi}$ , a predetermined data loss rate could always be either higher or lower than that calculated by Eq. (15). In this case, if the predetermined data loss rate  $\psi'$  is higher, i.e.,  $\psi' > \psi$ , then a number of clusters can achieve the sinking ratio  $\frac{1}{1+\psi'}$  while the sinking ratio of the rest of clusters might be much less than  $\frac{1}{1+\psi}$ . On the other hand, if the predetermined data loss rate  $\psi'$  is lower, i.e.,  $\psi' < \psi$ , then the maximum sinking ratio for each cluster is still  $\frac{1}{1+\psi}$ . That suggest the correctness of the data loss rate utilizing Eq. (15).

**Theorem 1.** The established partition is the optimal one.

Fig. 1. All nodes of  $H_S$  on  $CH_S$ .Fig. 2. At least one node of  $H_S$  not on  $CH_S$ .

**Proof.** Let the partition  $P' = \{C_i\}$  discovered on the set  $S$  in a greedy searching manner along the  $H_S$ , in which each pair of adjacent nodes  $s_i, s_{i+1} \in H_S$  are closest to each other i.e.  $L(s_i s_{i+j}) \geq L(s_i s_{i+1})$ ,  $j \geq 1$ , such that  $L(P')$  is minimum due to the satisfaction of Eq. (14). Then, we distinguish two cases to prove that each  $H_{C_i}$  is longer without searching along  $H_S$ .

**Case 1:**  $\forall s_i \in H_S, s_i \in CH_S$ .

In this case, we take two groups  $C_1$  and  $C_2$  shown in Fig. 1 as an example to prove this theorem, where  $s_1, s_k, s_{k+1} \in C_1$  and  $s_{k+m}, s_{k+m+1}, s_n \in C_2$ . Let each node be labeled clockwise as the searching order. Since each optimum UAV tour is constructed in a greedy searching manner, the fact that  $s_{k+m}$  not belonging to  $C_1$  implies  $L(s_k s_{k+1} \cup s_{k+1} s_{k+m} \cup s_{k+m} s_1 \cup s_1 s_k) > L(s_k s_{k+1} \cup s_{k+1} s_1 \cup s_1 s_k)$ . If the searching is proceeded not along the  $H_S$  (i.e.,  $s_{k+m}$  joins  $C_1$  earlier than  $s_{k+1}$ ), then we have  $L(s_k s_{k+m} \cup s_{k+m} s_{k+1} \cup s_{k+1} s_1 \cup s_1 s_k) > L(s_k s_{k+1} \cup s_{k+1} s_1 \cup s_1 s_k)$  such that Eq. (13) is not satisfied. That suggests either  $s_{k+1}$  or  $s_{k+m}$  should join  $C_2$ . If we add  $s_{k+m}$  to  $C_1$  and let  $s_{k+1}$  join  $C_2$ , which is  $C'_1 = C_1 \setminus \{s_{k+1}\} \cup \{s_{k+m}\}$  and  $C'_2 = C_2 \setminus \{s_{k+m}\} \cup \{s_{k+1}\}$ , then we have  $L(C'_1 \cup C'_2) > L(C_1 \cup C_2)$ . The reasons are as follows. For quadrilaterals  $s_{k+1} s_{k+m} s_1 s_n$  and  $s_k s_{k+1} s_{k+m} s_{k+m+1}$ , we have  $L(s_{k+1} s_n \cup s_{k+m} s_1) > L(s_1 s_{k+1} \cup s_{k+m} s_n)$  and  $L(s_k s_{k+m} \cup s_{k+1} s_{k+m+1}) > L(s_k s_{k+1} \cup s_{k+m} s_{k+m+1})$  respectively.

**Case 2:**  $\exists s_i \in H_S, s_i \notin CH_S$  as shown in Fig. 2.

Similarly, we can deduce that  $L(P'_1 \cup P'_2) > L(C_1 \cup C_2)$ . ■

**Theorem 2.** For a partition  $P'$ , we have  $\gamma = \frac{L(P')}{L(P)}$ , where  $\gamma \in (1.5, 2)$ .

**Proof.** For any connected graph, there is a minimal Steiner tree  $T = \cup T_i$ , where each  $T_i$  is a full Steiner tree, such that each Steiner point in  $T_i$  has a degree between 3 and 5. In addition, we can transform a full Steiner tree into the one of 3 degree Steiner points such that each angle at a Steiner point is exactly  $120^\circ$ . We call such tree a 3 full Steiner tree. Suppose  $P'$  is connected by a minimal Steiner tree  $T$  such that for each  $C_i \in P'$  there exist two nodes  $s_i, s_j \in C_i$  adjacent to a Steiner point  $p_i$  with  $d_{s_i, p_i} = d_{s_j, p_i} = R$ . Then, we are going to take Fig. 3 to complete the proof.

For an optimum grouping  $P$ , there exist at least two clusters, say  $C_1^* = \{s_i | 1 \leq i \leq k\}$  and  $C_2^* = \{s_j | k+3 \leq j \leq k+m\}$ , such that

$C_1^*$  and  $C_2^*$  are connected by the minimal Steiner  $T$  with two Steiner points  $s_{k+1}$  and  $s_{k+2}$  of degree 3 as shown in Fig. 3(a). Then we have  $L(P) = L(H_{C_1^*}) + L(H_{C_2^*})$ . Let the 3-full Steiner tree connecting to  $C_1^*$  possess longest edges  $s_1 s_{k+1} = s_k s_{k+1} = R$ . Note that  $H_{C_1^*}$  and  $H_{C_2^*}$  are optimum UAV tours. Here, we assume the distance  $d(s_i, s_j)$  between each pair of nodes  $s_i$  and  $s_j$  is beyond the communication range  $r$ , then we have  $d(s_i, s_j) \geq r + \epsilon$  where  $\epsilon$  is negligible. Since  $\angle s_1 s_{k+1} s_k = 120^\circ$ , then it is easy to get  $s_1 s_k = \sqrt{3}R$ . Let  $L$  denote the longest distance between each pair of points within the deployment area. It is obviously that  $s_1 s_{k+3} \leq L$  and  $s_k s_{k+3} \leq L$ . If  $k \rightarrow \infty$ , then  $s_{k-1}$  is infinitely closed to  $s_k$  such that we have  $s_{k-1} s_{k+3} \leq L$ . If we add  $s_k$  to  $C_2$  and let  $s_{k+3}$  join  $C_1$ , which is  $P'_1 = C_1 \setminus \{s_k\} \cup \{s_{k+3}\}$  and  $P'_2 = C_2 \setminus \{s_{k+3}\} \cup \{s_k\}$ , then we have  $L(P') = L(H_{C'_1}) + L(H_{C'_2})$ ,  $H_{P'_1} > H_{C_1^*}$  and  $H_{P'_2} > H_{C_2^*}$ . The reasons behind that are as follows. According to the structure of  $H_{P'_1}$  and  $H_{C_1^*}$ , we have

$$\begin{aligned} L(H_{C_1^*}) &\geq (r + \epsilon)(k - 1) + \sqrt{3}R \\ &> r(k - 1) + \sqrt{3}R \\ L(H_{C'_1}) &\leq 2L + (k - 2)r. \end{aligned} \quad (16)$$

Let the function  $f(k) = \frac{2L + (k-2)r}{r(k-1) + \sqrt{3}R}$  denote the approximation ratio between  $L(H_{P'_1})$  and  $L(H_{P_1})$ . Then, we have  $f(k)' = (k - 1)r^2 + \sqrt{3}Rr - (k - 2)r^2 - 2Lr$ . Since  $\frac{L}{r} + 1 \geq k$  and  $\sqrt{3}R \leq L$ , it is easy to verify  $f'(k) < 0$ . That implies  $f(k)$  is a monotonic decreasing function. Since  $3 \leq |C_i| \leq \frac{L}{r} - 1$ , then we have

$$\begin{aligned} f(k) &= \frac{L}{r} - 1 = \frac{3L - r}{\sqrt{3}R + L} \\ &< f(k) \\ &< \frac{2L + r}{\sqrt{3}R + 2r} = f(k = 3). \end{aligned} \quad (17)$$

It can be deduced  $f(k) \in (1.5, 2)$  due to  $\lim_{L \rightarrow \infty} \frac{2L+r}{\sqrt{3}R+2r} = 2$  and  $\lim_{L \rightarrow \infty} \frac{3L-r}{\sqrt{3}R+L} = 1.5$ . Similarly, we have  $f(k') \in (1.5, 2)$ , where  $f(k')$  denotes the approximation ratio between  $L(H_{P'_2})$  and  $L(H_{P_2})$ . Therefore, the theorem holds. ■

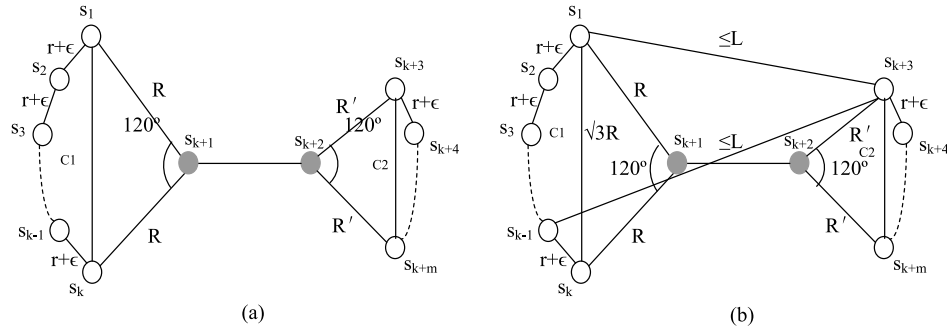


Fig. 3. An optimum partition vs. a suboptimal partition.

In addition, the optimal partition should take the energy cost into consideration. In order to approximate the real energy cost of a certain partition, we first introduce the probability density functions (pdf) of the distribution of different terrains. From the global perspective, the energy cost for each cell  $c$  should consider the pdf of the corresponding terrain  $p_c$  as

$$F'_c = \int_{l_c} \int_{e_c} r_c p_c. \quad (18)$$

Then, we define the **Approximated Route Energy Efficiency** as the proportion between aggregated data and corresponding energy cost. Obviously, the optimal partition should be the one of the maximal overall approximated energy efficiency. In addition, if two partition has the same approximated energy efficiency, then we choose the one with less energy cost. This is because more aggregated data requires more aggregation time due to the limited data collection rate. That indicates more aggregation time is required such that the sinking ratio drops. Although, each cluster of the optimal partition is assigned a UAV for data collection and aggregation, in which the energy efficient route within each cluster should be discovered.

#### 4.3. DQN based UAV route design

We design the UAV route utilizing a deep reinforcement learning (DRL) [18] based technology DQN to increase the sinking ratio and reduce the energy cost. The basic idea of applying DQN for UAV route design is to give an action  $a_t^u$  to the state  $s_t^u$  of UAVs at time slot  $t$  and receive the reward  $r_t^u$  and the next state  $s_{t+1}^u$ . Therefore, we need to define the state space, the action space, and the reward, respectively.

1. **State:** Each state is consist of three important components, tasks of corresponding security level *task*, positions of UAVs *position*, remaining tasks *remainingtask* required to be completed, that is  $S = \{(task, position, remainingtask)\}$ ;
2. **Action:** For each UAV, only 8 directions *dir* are considered, i.e., East, South, West, North, Northeast, Northwest, Southeast, and Northwest; In addition, we assume at each time slot the travel distance of a UAV *dis* is less than a maximum value  $dis_{max}$ ; That suggest each action can be written as  $a_t = \{dir_t, dis_t\}$ ;
3. **Reward:** Once the  $i$ th UAV is employed to perform data aggregation tasks of different security levels, the ratio between the amount of data *data* collected and the energy consumed  $Energy_{i,T}$  on route  $T$  and the proportion of the completed tasks in overall tasks are considered as:

$$r_t^u = \begin{cases} \frac{1}{Energy_{i,T}}, & \text{if } data = 0 \\ \frac{data * task}{remainingtask * Energy_{i,T}}, & \text{otherwise,} \end{cases}$$

where the energy consumption  $Energy_{i,T}$  is calculated within a time interval rather than that consumed on the entire route  $T$ . Then, the reward for all UAVs can be rewritten as  $r_t = \sum_i r_t^u$ .

Note that once an action is chosen utilizing  $\epsilon$ -greedy policy based on current state. Then the reward is obtained and the next state is observed from the environment [17]. Different from the traditional DQN, only the excellent experience, which possesses a reward higher than the average reward of latest  $M$  time slot can be store in the experience pool in terms of a transition  $(s_i, a_i, r_i, s_{i+1})$ , instead of the ordinary experience. This is because excellent experiences are supposed to contain more useful information about the interactions between UAVs and the environment. That suggest learning from excellent experiences can stabilize the learning process and accelerate the convergence.

In the training of DQN, we give the discount factor  $\delta \in (0, 1]$ , which shows how uncertain the rewards are. Then, we update Q network utilizing gradient descent w.r.t parameter  $\theta$  based on the loss function  $\mathcal{L}$  with a minibatch randomly sampled transitions  $(s_i, a_i, r_i, s_{i+1})$  as follows:

$$\mathcal{L} = [(r_i + \delta Q(s_{i+1}, a_{i+1} | \theta^-) - Q(s_i, a_i | \theta))^2], \quad (19)$$

where  $\theta^-$  represents the parameter of target network  $\hat{Q}$ . Next, we update the  $\hat{Q}$  for every  $C$  steps by

$$\hat{Q} = Q. \quad (20)$$

Based on the  $\epsilon$ -greedy policy, we choose the optimal action to maximize the utility with probability  $1 - \epsilon$ . To stabilize the learning process of DQN, we consider the parameter  $\epsilon$  a time-varying one. In the beginning of the learning process, the parameter  $\epsilon$  should be set a little bit larger for deep exploration. However, when the learning process tends to converge, the parameter  $\epsilon$  should decrease exponentially due to the optimal action has been found for each state to ensure the convergence of the learning process. Eventually, the optimal action  $a^*$  is chosen by

$$a^* = \arg \max Q(s, a) \quad (21)$$

We summarize the UAV route design with DQN in Algorithm 1.

---

#### Algorithm 1 UAV route design with DQN

---

```

for  $n = 1, 2, 3, \dots$  do
  Select the action  $a_n$  via  $\epsilon$ -greedy policy
  Execute action  $a_n$ 
  Observe  $s_{n+1}$  and Calculate  $r_n$ 
  Store excellent transition  $(s_n, a_n, r_n, s_{n+1})$  in the experience pool
only
  Sample a mini-batch of transitions  $(s_i, a_i, r_i, s_{i+1})$  randomly from experience pool
  Update  $Q(s_i, a_i)$  via (19)
  Update  $\hat{Q}$  via (20) for every  $C$  steps
end for

```

---

## 5. Performance evaluation

### 5.1. Simulation setup

We conduct the experiments of IDAA considering the scenario shown in Fig. 4. There are three type of tasks of different security



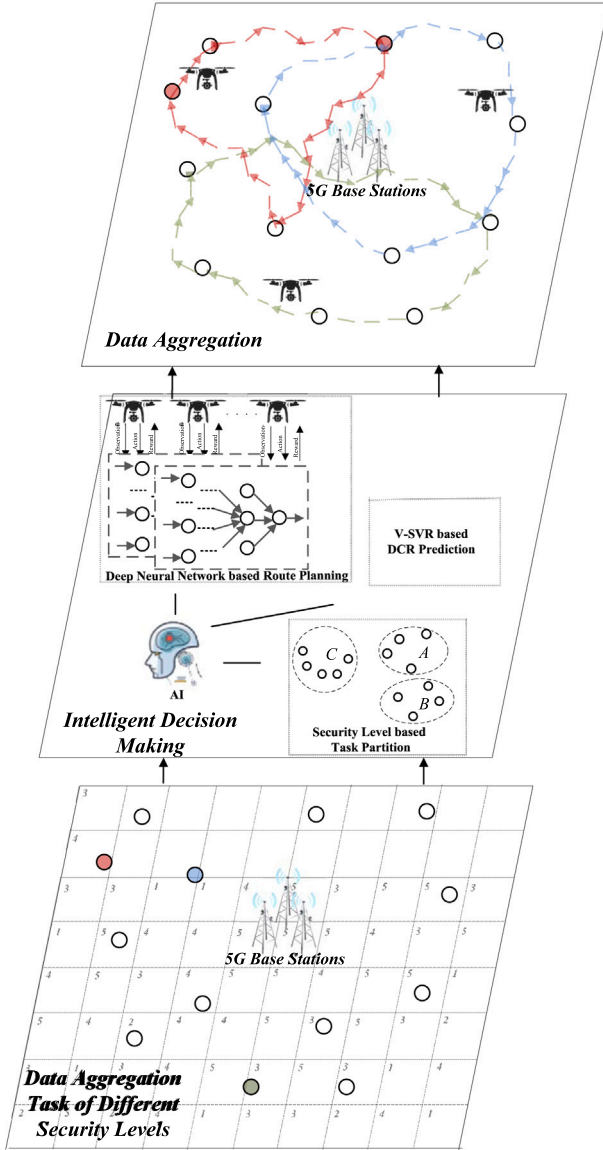


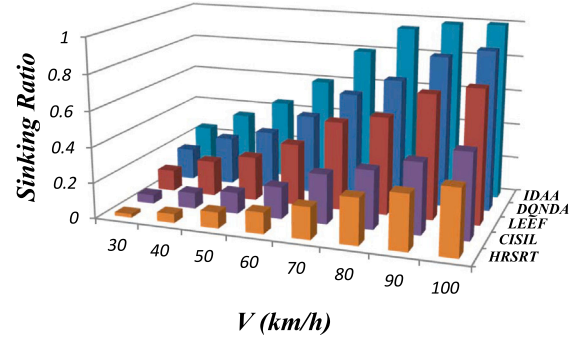
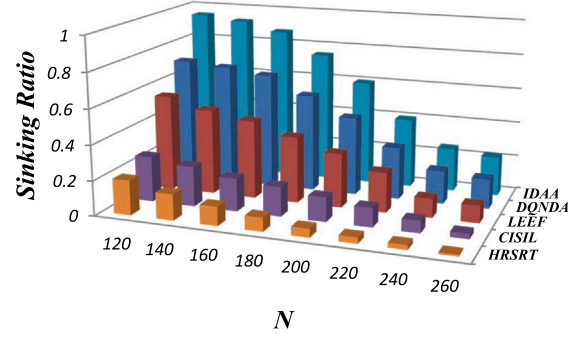
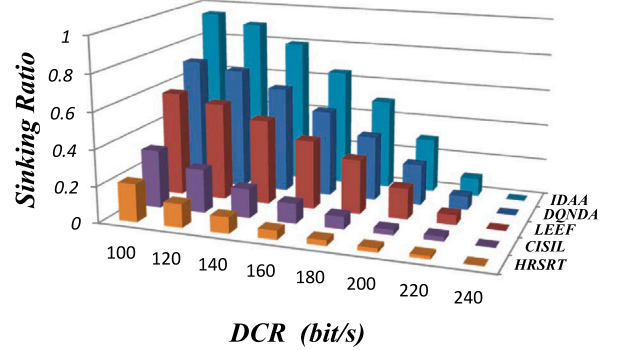
Fig. 4. The performance evaluation scenario of proposed IDAA.

levels High, Medium and Low, each type of which are represent in red dots, blue dots and green dots, respectively. With the intelligent decision making, i.e., DQN based UAV route planning, v-SVR based DCR prediction, and security level based task partition, UAVs aggregate data from sensors w.r.t the corresponding security levels toward the 5G base stations. The experiment is implemented in Python on an Intel Core i7 8550U, 62GB RAM computer. In addition, sensors are assumed to be deployed within  $3000 \text{ m} \times 3000 \text{ m}$  area of complex terrains. We give parameters of this experiment in Table 1.

We compare IDAA with CISIL [1], LEF [2], DQND [10], and HRSRT [19] in energy cost and sinking ratio.

## 5.2. Sinking ratio

The reverse effects on sinking ratio by velocity  $V$  are shown in Fig. 5. It is obviously that with the growth of  $V$  the sinking ratio rises for all approaches. IDAA obtains the highest sinking ratio. The reason behind that is we employ DQN for UAV route design to increase the sinking ratio and reduce the energy cost.

Fig. 5. Sinking ratio on different  $V$ .Fig. 6. Sinking ratio on different  $N$ .Fig. 7. Sinking ratio on different  $DCR$ .

See from Fig. 6, it is clear that with the increment of sensors  $N$  the sinking ratio drops for all approaches. This is because more sensors contributes to further distance to aggregate data with insufficient time. When the area is densely populated with sensors, the distance is shortened. IDAA performs better than baselines.

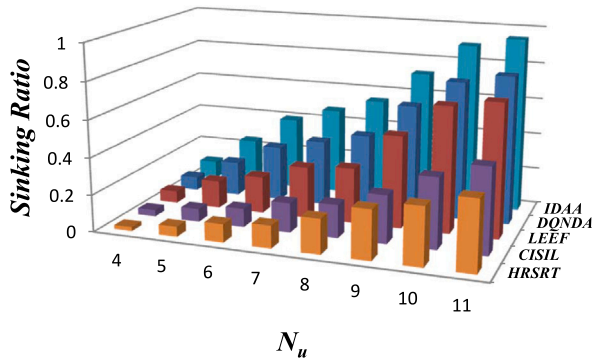
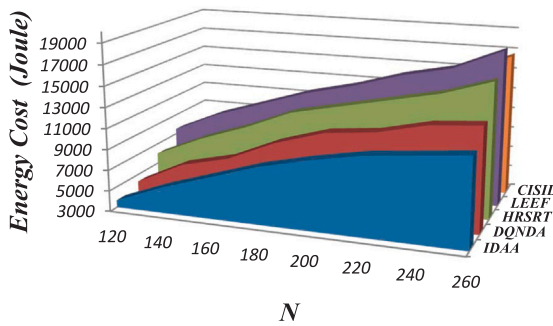
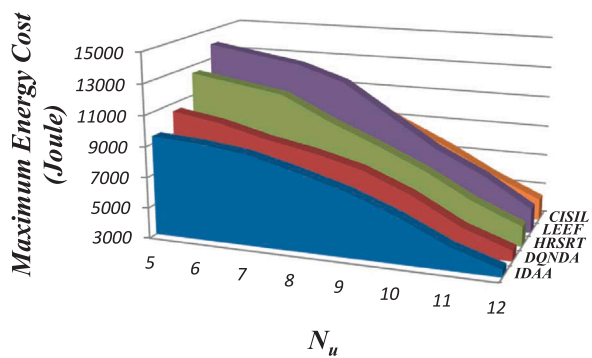
Observed from Fig. 7, the sinking ratio drops with the growth of data collection rate  $DCR$ . Recall that (13) describes the tradeoff of  $DCR$  and sinking ratio. It is no doubt that the sinking ratio drops if  $DCR$  is set too high. As shown in Fig. 7, the sinking ratio reaches the highest value when  $DCR = 120 \text{ bit/s}$  compared with the lowest value when  $DCR = 260 \text{ bit/s}$ . All baselines obtains less sinking ratios compared with IDAA.

The impact of the number of UAVs  $N_u$  on the sinking ratio is shown in Fig. 8. It is clearly that the increment of  $N_u$  results in the growth of the sinking ratio. This is because more UAVs with corresponding security levels will collect more data. However, the experiment is conducted in a fixed size area that 100% sinking ratio can be achieved without further UAV deployment. IDAA still outperforms baselines with the highest sinking ratio.

**Table 1**

Simulation setup.

Parameter	Value
Communication range $R$	[10, 50] m
Number of UAV $N_u$	[5, 12]
Speed of UAV $V$	[1, 8] m/s
Rotating angle $A_\theta$	[45°, 90°, 135°, 180°]
Energy level of UAV at Start Time	100 Wh
Sensitivity of receiver	-100 dBm
Bit Rate	120 kbps
Frequency of transmission	2.45 GHZ
Energy coefficient $\mu$	50 J/m
Risk of terrain $r_c$	[0.005, 1]
Elevation of terrain $e_c$	[0, 3] m

**Fig. 8.** Sinking ratio on different  $N_u$ .**Fig. 9.** Energy cost w.r.t  $N$ .**Fig. 10.** Maximum energy cost w.r.t different  $N_u$ .

### 5.3. Energy cost

Fig. 9 shows the impact of  $N$  on energy cost. It is straightforward that more tasks results in more energy cost. See from Fig. 10, we know that the maximum energy decreases if  $N_u$  increases. The IDAA

outperforms baselines in both energy cost and maximum energy cost. Furthermore, IDAA is affected by  $N_u$  much less compared with other strategies due to DQN based UAV route design for energy efficiency.

## 6. Conclusion

Unmanned Aerial Vehicle (UAV) has become an important part of 5G communication, and is used in various scenarios, i.e., cargo delivery, agricultural application, event surveillance, etc. In this paper, an Intelligent UAV based Data Aggregation Strategy, named (IDAA), is proposed for 5G-enabled IoT. Specifically, IDAA employs an v-SV regression to predict the data collection rate. Then, a security level based task partition is adopted. Eventually, a deep reinforcement learning based UAV route design is implemented for energy efficiency. The theoretical analysis and simulations indicate that IDAA obtains a higher sinking ratio and a lower energy cost while compared with contemporary strategies.

### CRedit authorship contribution statement

**Xiaoding Wang:** Performed sample preparation and data analysis. **Sahil Garg:** Supervision. **Hui Lin:** Developed mechanics modeling and analysis. **Georges Kaddoum:** Performed sample preparation and structure fabrication. **Jia Hu:** Performed calculations. **Mohammed F. Alhamid:** Performed simulations using classical force fields.

### Declaration of competing interest

The authors declare that they have no known competing financial interests or personal relationships that could have appeared to influence the work reported in this paper.

### Acknowledgment

The authors are grateful to the Deanship of Scientific Research at King Saud University, Riyadh, Saudi Arabia for funding this work through the Vice Deanship of Scientific Research Chairs: Chair of Smart Technologies. All authors read and contributed to the manuscript.

### References

- [1] W. Lalouani, M. Younis, N. Badache, Interconnecting isolated network segments through intermittent links, *J. Netw. Comput. Appl.* 108 (2018) 53–63.
- [2] S. Lee, M. Younis, B. Anglin, M. Lee, LEEF: Latency and energy efficient federation of disjoint wireless sensor segments, *Ad Hoc Netw.* 71 (2018) 88–103.
- [3] Y.K. Joshi, M. Younis, Restoring connectivity in a resource constrained WSN, *J. Netw. Comput. Appl.* 66 (2016) 151–165.
- [4] L. Goratti, T. Baykas, T. Rasheed, S. Kato, NACRP: A connectivity protocol for star topology wireless sensor networks, *IEEE Wirel. Commun. Lett.* 5 (2) (2016) 120–123.
- [5] Z. Xu, L. Chen, C. Chen, X. Guan, Joint clustering and routing design for reliable and efficient data collection in large-scale wireless sensor networks, *IEEE Internet Things J.* 3 (4) (2016) 520–532.
- [6] A. Abbas, M. Younis, Establishing connectivity among disjoint terminals using a mix of stationary and mobile relays, *Comput. Commun.* 36 (13) (2013) 1411–1421.
- [7] X. Wang, L. Xu, S. Zhou, W. Wu, Hybrid recovery strategy based on random terrain in wireless sensor networks, *Sci. Program.* 2017 (2017) article id. 5807289.
- [8] I.F. Senturk, K. Akkaya, S. Jananefat, Towards realistic connectivity restoration in partitioned mobile sensor networks, *Int. J. Commun. Syst.* 29 (2) (2016) 230–250.
- [9] J. Wang, H. Zhang, Z. Ruan, T. Wang, X.D. Wang, A machine learning based connectivity restoration strategy for industrial IoTs, *IEEE Access* 8 (2020) 71136–71145.
- [10] K. Toyoshima, T. Oda, M. Hirota, K. Katayama, L. Barolli, A DQN based mobile actor node control in WSN: Simulation results of different distributions of events considering three-dimensional environment, in: *International Conference on Emerging Internetworking, Data and Web Technologies*, Springer, Cham, 2020, pp. 197–209.

- [11] D. Zorbas, L.D.P. Pugliese, T. Razafindralambo, F. Guerriero, Optimal drone placement and cost-efficient target coverage, *J. Netw. Comput. Appl.* 75 (2016) 16–31.
- [12] E. Tuba, R. Capor-Hrosik, A. Alihodzic, M. Tuba, Drone placement for optimal coverage by brain storm optimization algorithm, in: *Proc. Int. Conf. Health Inf. Sci.*, Springer, Cham, Switzerland, 2017, pp. 167–176.
- [13] H. Shakhathreh, A. Khreishah, Optimal placement of a UAV to maximize the lifetime of wireless devices, 2018, [Online]. Available: <https://arxiv.org/abs/1804.02144>.
- [14] A. Rodriguez, A. Gutierrez, L. Rivera, L. Ramirez, RWA: Comparison of genetic algorithms and simulated annealing in dynamic traffic, in: *Proc. Adv. Comput. Commun. Eng. Technol.*, Springer, Cham, Switzerland, 2015, pp. 3–14.
- [15] C.H. Liu, Z. Chen, J. Tang, J. Xu, C. Piao, Energy-efficient UAV control for effective and fair communication coverage: A deep reinforcement learning approach, *IEEE J. Sel. Areas Commun.* 36 (9) (2018) 2059–2070.
- [16] J. Wang, J. Hu, G. Min, W. Zhan, Q. Ni, N. Georgalas, Computation offloading in multi-access edge computing using a deep sequential model based on reinforcement learning, *IEEE Commun. Mag.* 57 (5) (2019) 64–69.
- [17] J. Wang, J. Hu, G. Min, A. Zomaya, N. Georgalas, Fast adaptive task offloading in edge computing based on meta reinforcement learning, *IEEE Trans. Parallel Distrib. Syst.* 32 (1) (2021) 242–253.
- [18] X. Guo, H. Lin, Z. Li, M. Peng, Deep reinforcement learning based QoS-aware secure routing for SDN-IoT, *IEEE Internet Things J.* 7 (7) (2020) 6242–6251.
- [19] X. Wang, S. Garg, H. Lin, G. Kaddoum, J. Hu, M.S. Hossain, A secure data aggregation strategy in edge computing and blockchain empowered internet of things, *IEEE Internet Things J.* (2020) <http://dx.doi.org/10.1109/JIOT.2020.3023588>.
- [20] L. Ding, D. Zhao, H. Ma, H. Wang, L. Liu, Energy-efficient min-max planning of heterogeneous tasks with multiple uavs, in: *2018 IEEE 24th International Conference on Parallel and Distributed Systems, ICPADS, 2018*, pp. 339–346.



**Xiaoding Wang** received his Ph.D. in College of Mathematics and Informatics from Fujian Normal University in 2016, he is an Associate Professor with the School of Fujian Normal University, China. His main research interests include network optimization and fault tolerance.



**Sahil Garg** (Member, IEEE) is currently working as a Postdoctoral Research Fellow with Department of Electrical Engineering, École de technologie supérieure, Université Québec, Montreal, Canada. His research interests include Machine Learning, Big Data Analytics, Knowledge Discovery, Cloud Computing, Internet of Things, Software Defined Networking, and Vehicular Ad hoc Networks. Some of his research findings are published in top-tier journals and various International conferences. He was the recipient of prestigious Visvesvaraya Ph.D. fellowship from the Ministry of Electronics & Information Technology under Government of India (2016/2018). For his research, he also received the IEEE ICC best paper award in 2018 at Kansas City, USA. He serves as the Managing Editor of Springer's Human-centric Computing and Information Sciences (HCIS) journal. He is also an Associate Editor of IEEE Network Magazine, Elsevier's Future Generation Computer Systems (FGCS), and Wiley's International Journal of Communication Systems (IJCS). In addition, he also serves as the Workshops and Symposia Officer of the IEEE ComSoc Emerging Technology Initiative on Aerial Communications. He has guest edited a number of Special Issues in top-cited journals including IEEE T-ITS, IEEE TII, the IEEE IoT Journal, IEEE Network



**Hui Lin** is a professor in the College of Mathematics and Informatics at the Fujian Normal University, Fuzhou, China. He received his Ph.D. degree in Computing System Architecture from College of Computer Science of the Xidian University, China, in 2013. Now he is a M.E. supervisor in College of Mathematics and Informatics at Fujian Normal University, Fuzhou, China. His research interests include mobile cloud computing systems, blockchain, and network security. He has published more than 50 papers in international journals and conferences.



**Georges Kaddoum** Prof. Kaddoum is the recipient of the Research Excellence Award of the University du Quebec, 2018" and the Research Excellence Award emerging researcher" from TS, 2019. Additionally, he is a co-recipient of the Best Papers Awards of the IEEE PIMRC 2017 and the IEEE WiMob 2014. Moreover, he received the "Exemplary Reviewer Award" from IEEE trans. on comm. Twice in 2015 and 2017. He is currently serving as an associate editor for the IEEE trans. on information forensics and security and the IEEE comm. Letters. Prof. Kaddoum held the TS Research Chair in physical-layer security for wireless networks. He published over 200 journal and conference papers and two pending patents. He received his Ph.D. with honor in signal processing and telecommunications from the National Institute of Applied Sciences, Toulouse, France, 2008.



**Jia Hu** is a Senior Lecturer in Computer Science at the University of Exeter. He received his PhD in Computer Science from the University of Bradford, UK, in 2010, and M.Eng. and B.Eng degrees in Electronic Engineering from Huazhong University of Science and Technology, Wuhan, China, in 2006 and 2004, respectively. His research interests include edge-cloud computing, resource optimization, applied machine learning, and network security. He has published over 70 research papers within these areas in prestigious international journals and reputable international conferences. He serves on the editorial board of Elsevier Computers & Electrical Engineering and has guest-edited many special issues on major international journals (e.g., IEEE IoT journal, Computer Networks, Ad Hoc Networks). He has served as General Chair/Co-Chair of IEEE CIT'15, IUCC'15, etc., and Program Chair/Co-Chair of IEEE ISPA'20, ScalCom'19, SmartCity'18, CYBCONF'17, EAI SmartGIFT'2016, etc. He has been the recipient of the Best Paper Awards at IEEE SOSE'16 and IUCC'14.

**Mohammed F. Alhamid** received his Master and Ph.D. degrees in Computer Science from the School of Electrical Engineering and Computer Science at the University of Ottawa, Canada. Dr. Alhamid is currently an Assistant Professor of Software engineering, college of computer and information sciences, King Saud University, Riyadh, Saudi Arabia. His research interest includes Machine Learning, AI, Social Computing, Internet-of-Things, and e-commerce/FinTech application. He is a member of IEEE.